International Journal of Mass Spectrometry 308 (2011) 56–64

Contents lists available at ScienceDirect

International Journal of Mass Spectrometry

journal homepage: www.elsevier.com/locate/ijms

Electrospray tandem mass spectrometry of poly(amino)ester dendrimers: Dissociation rules and structural characterization of defective molecules

Aura Tintaru[a], Christophe Chendo[b], Valérie Monnier[b], Camille Bouillon[c], Gilles Quéléver[c], Ling Peng[c], Laurence Charles[a,*]

[a] Universités Aix-Marseille I, II & III–CNRS, UMR 6264: Laboratoire Chimie Provence, Spectrométries Appliquées à la Chimie Structurale, F-13397 Marseille Cedex 20, France
[b] Fédération des Sciences Chimiques, Spectropole, FR1739, Universités d'Aix-Marseille I, II et III–CNRS, Av. Escadrille Normandie-Niemen, 13397 Marseille Cedex 20, France
[c] Centre Interdisciplinaire de Nanoscience de Marseille, Université de la Méditerranée, Faculté des Sciences de Luminy, UPR CNRS 3118, 13288 Marseille Cedex 9, France

ARTICLE INFO

Article history:
Received 2 May 2011
Received in revised form 20 July 2011
Accepted 20 July 2011
Available online 26 July 2011

Key words:
Dendrimers
Poly(amino)ester
Structural characterization
CID
Defective molecules

ABSTRACT

A poly(amino)ester dendrimer, bearing *tert*-butyl ester terminations and used as the precursor of an acid-terminating poly(amino)ester dendrimer, was studied by electrospray ionization tandem mass spectrometry to establish its fragmentation rules upon collision-induced dissociation. Mechanisms for dissociation reactions experienced by protonated molecules were proposed and supported by accurate mass measurements. The release of 2-methylprop-1-ene was observed as many times as *tert*-butyl groups were available. Each of these steps was followed by elimination of carbon dioxide and ethylene within the so-deprotected branches. Detachment of an entire arm, released as a neutral or as a protonated molecule, was found to be a useful complementary process but it mainly proceeded from the singly charged precursor. Three targeted dendritic impurities were structurally characterized by monitoring the occurrence of these reactions together with any deviation from the reference behavior. Detection of these compounds in the precursor sample could account for the presence of defective molecules previously characterized in the acid-terminating poly(amino)ester dendrimer sample.

© 2011 Elsevier B.V. All rights reserved.

1. Introduction

Synthetic dendrimers have attracted considerable attention as ideal drug delivery nanovehicles in biomedical applications, thanks to their unique properties of well defined structure alongside with a large number of terminal groups located on the surface, allowing high drug payload confined in a small volume. Among various dendrimers evaluated for their application as drug delivery systems, polyester dendrimers are promising biodegradable candidates as safe and efficient delivery devices, because they are expected to be rapidly degraded via ester hydrolysis, and hence eliminated from the cell after the delivery process [1]. Fréchet et al. reported polyester scaffold based dendrimers which have been shown to be non-toxic even at very high concentrations [2,3]. As an alternative to polyesters, poly(amino)ester dendrimers have further advantage to contain amine functionalities which can serve as buffers to neutralize the acids generated from the ester hydrolysis, offering a benign and non-aggressive microenvironment during dendrimer degradation.

However, the synthesis of poly(amino)ester dendrimers remains challenging. When using Michael addition of amines to produce amine-bearing dendrimers, the ester groups may be affected by the nucleophilic attack of the amines. In addition, the presence of amine functionalities in poly(amino)ester leads to general problems encountered during the synthesis of various amine-containing esters [4,5], when using conventional methods. A new strategy has recently been reported to synthesize amine-bearing esters via activated cyanomethyl ester intermediates [5], and has been explored for the preparation of poly(amino)ester dendrimers [6]. This approach consists of four consecutive reactions (Scheme 1), namely: (1) activation of acidic terminals as cyanomethyl esters, (2) transesterification with an excess of alcohol bearing ester terminals and a tertiary amine as branching unit followed by (3) scavenging of the excess of alcohol using benzoic anhydride, and (4) deprotection of the ester terminals to generate acidic functionalities using trifluoroacetic acid. Repetition of these four iterative steps leads to the construction of higher generation dendrimers.

The so-synthesized dendrimers were recently studied using tandem mass spectrometry to investigate any structural imperfections [7]. While the high symmetry of dendritic structures, combined with usually low amounts of defective molecules, is usually a drawback in nuclear magnetic resonance analysis, it

* Corresponding author. Tel.: +33 491 28 8678; fax: +33 491 28 2897.
E-mail address: laurence.charles@univ-provence.fr (L. Charles).

1387-3806/$ – see front matter © 2011 Elsevier B.V. All rights reserved.
doi:10.1016/j.ijms.2011.07.021

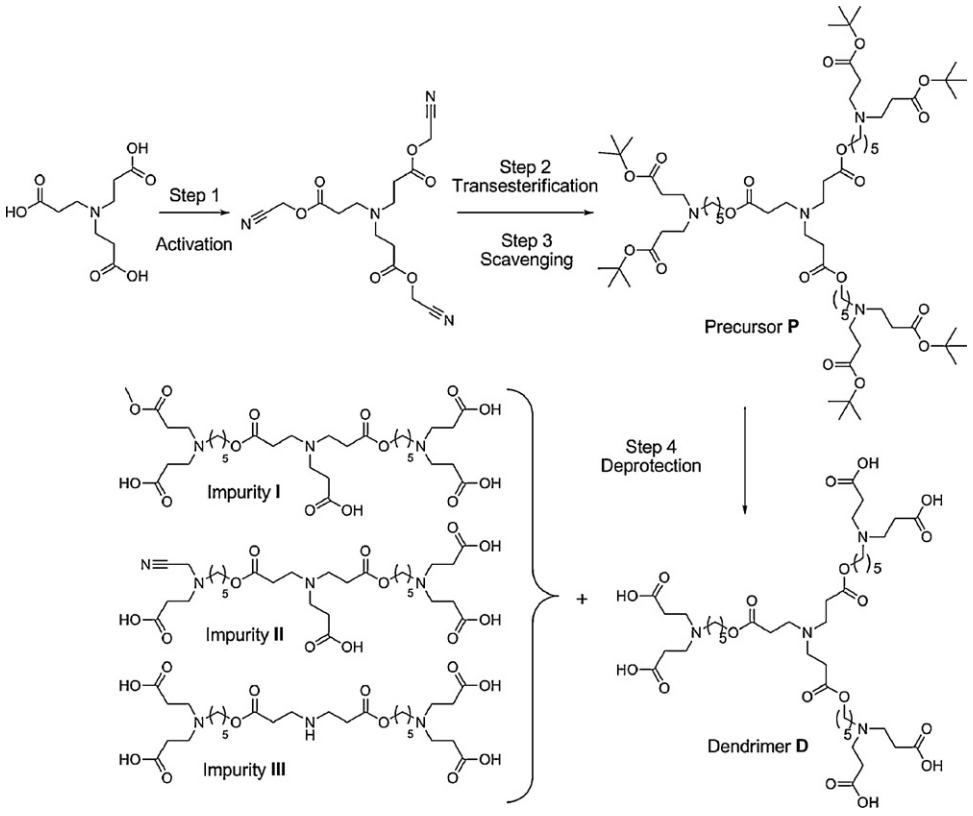

Scheme 1. Synthesis of the poly(amino)ester dendrimer **D** with acidic terminations via the *tert*-butyl-terminated dendritic precursor **P**, and minor impurities detected in the **D** sample.

allows straightforward information to be rapidly obtained in mass spectrometry. Indeed, simple dissociation rules can usually be established from intact molecular adducts generated by soft ionization techniques, such as electrospray (ESI) and matrix-assisted laser desorption/ionization (MALDI), and subjected to collision-induced dissociations (CID) [8–13] or post-source decay (PSD) [10,11,14] experiments. The first generation of acid-terminating poly(amino)ester dendrimer could be ionized in both polarity modes, but the most structurally relevant dissociation pathways were found from the deprotonated molecule. Three main defective molecules (Scheme 1) have been identified as minor impurities, based on deviation of their CID behavior as compared to the reference MS/MS pattern of the perfect **D** molecule [7].

The aim of the present study was to scrutinize the dendrimer produced in the preceding synthesis step (designated as **P**, the precursor of **D**, in Scheme 1) for any impurities which could explain formation of defective molecules in the final dendrimer sample **D**. Dendrimer **P** is a poly(amino)ester dendrimer bearing *tert*-butyl ester terminations, of which the dissociation behavior under collisional activation needs to be first established. It will then serve as a reference for structural characterization of the possibly related impurities present in **P**.

2. Materials and methods

2.1. Chemicals

HPLC-grade methanol was from SDS (Peypin, France) and used without further purification. Ammonium acetate, as well as poly(ethylene oxide) and poly(propylene glycol) of various sizes used for mass calibration, were purchased from Sigma–Aldrich (St. Louis, MO) and were used as received.

2.2. Mass spectrometry

High resolution MS and MS/MS experiments were performed with a QStar Elite mass spectrometer (Applied Biosystems SCIEX, Concord, ON, Canada) equipped with an electrospray ionization source operated in the positive ion mode. The capillary voltage was set at +5500 V and the cone voltage at +80 V. In this hybrid instrument, ions were measured using an orthogonal acceleration time-of-flight (oa-TOF) mass analyzer. A quadrupole was used for selection of precursor ions to be further submitted to collision induced dissociation (CID) in MS/MS experiments. In MS, accurate mass measurements were performed using two reference ions from a poly(ethylene glycol) or a poly(propylene glycol) internal standard, according to a procedure described elsewhere [15]. The precursor ion was used as the reference for accurate measurements of product ion *m/z* value in MS/MS spectra. MS^3 experiments were performed using a 3200 Q-TRAP mass spectrometer (Applied Biosystems SCIEX), equipped with an electrospray ionization source operated in the positive mode. The capillary voltage was set at +5500 V and the cone voltage at +80 V. Primary precursor ions generated in the ion source were selected in the quadrupole analyzer and submitted to CID in a collision cell. Secondary precursor ions produced during collisions were selected and then fragmented in a linear ion trap. In both instruments, air was used as the nebulizing gas (10 psi) while nitrogen was used as the curtain gas (20 psi) as well as the collision gas. Collision energy was set according to the experiments. Instrument control, data acquisition and data processing of all experiments were achieved using Analyst software (QS 2.0 and 1.4.1 for the QqTOF and the QqTrap instruments, respectively) provided by Applied Biosystems. Sample solutions were introduced in the ionization source at a 5 $\mu L\,min^{-1}$ flow rate using a syringe pump.

3. Results and discussion

3.1. ESI–MS analysis of the precursor sample

Precursor **P**, which structure is reminded in the inset of Fig. 1, is a dendrimer composed of three arms connected to a central nitrogen atom. Each arm is terminated by a pair of branches capped by a *tert*-butyl ester function. The positive mode ESI mass spectrum of this sample showed that **P** is detected as singly (*m/z* 1257.9), doubly (*m/z* 629.4) and triply (*m/z* 420.0) protonated molecules, with the doubly charged species $[\mathbf{P}+2H]^{2+}$ being the most abundant ion (Fig. 1). Accurate mass measurements performed for $[\mathbf{P}+2H]^{2+}$ were associated with the expected elemental composition, $C_{66}H_{122}N_4O_{18}{}^{2+}$ (*m/z* 629.4372) with a relative error of +3.2 ppm.

Additional signals were also observed and could be assigned to different protonation states of three compounds, further named **α** (929.6 Da), **β** (882.6 Da) and **γ** (1128.8 Da). Lowering the declustering potential to acquire MS data did not strongly modify relative intensity of peaks, suggesting that detected signals actually indicate the presence of different molecules in the sample rather than "in-source" fragmentation of the protonated dendrimer **P**. Moreover, none of these ions could be detected during MS/MS of protonated **P** molecules, regardless of their charge state (*vide infra*). Compounds **α**, **β** and **γ** were structurally analyzed in MS/MS based on the reference CID behavior of protonated **P** in order to determine whether these three molecules were impurities arising from the synthesis of **P** and could account for the presence of defective molecules in the final acid-terminating dendrimer sample.

3.2. MS/MS study of singly protonated *P*

CID of singly protonated **P** first showed six successive eliminations of a 56 Da neutral (Fig. 2a), found to be a C_4H_8 molecule based on accurate mass data obtained for product ions at *m/z* 1201.8, *m/z* 1145.7, *m/z* 1089.7, *m/z* 1033.6, *m/z* 977.6 and *m/z* 921.5 (Supplementary Table S1). These ions were annotated A_i^+, with *i* being the number of 56 Da neutral losses experienced by the $[\mathbf{P}+H]^+$ precursor ion, hence named A_0^+. This main reaction proceeds from each dendrimer branch and would consist of a 1,5-proton transfer from the *tert*-butyl terminal group to the carbonyl oxygen, yielding an acidic-terminated branch upon elimination of 2-methylprop-1-ene (pathway (i) in Scheme 2a), as previously reported from side chains of poly(*tert*-butylmethacrylate) [16]. As the reaction is proposed to occur via a charge-remote mechanism, it could proceed as many times as *tert*-butyl ester functions are present in the dendritic precursor. However, since multiple reactions could be proposed to account for most secondary product ions observed in the MS/MS spectrum of $[\mathbf{P}+H]^+$ (*vide infra*), it was not possible to conclude whether 2-methylprop-1-ene molecules are randomly eliminated, and various isomers are most probably generated for A_{2-4}^+.

The so-formed A_{1-6}^+ product ions bearing at least one acid-terminated branch, they were expected to eliminate a 72 Da neutral loss, as established for acid-terminating poly(amino)ester dendrimers [7]. This reaction could proceed via a concerted elimination of carbon dioxide and ethylene after a 1,5-proton transfer of the acidic proton to the nitrogen atom or, alternatively, via the loss of acrylic acid as depicted in Scheme 2a. This 72 Da neutral loss is observed to occur from all A_{1-6}^+ ions, yielding secondary product ions respectively observed at *m/z* 1129.8, *m/z* 1073.7, *m/z* 1017.7, *m/z* 961.6, *m/z* 905.5 and *m/z* 849.5 in Fig. 2a. These ions were annotated B_i^+, with *i* indicating the A_i^+ ion they arise from. Further elimination of up to $(i-1)$ 72 Da neutrals from B_{2-6}^+ ions was detected with increasing abundance as *i* increases.

An alternative fragmentation reaction from $[\mathbf{P}+H]^+$ would consist of the detachment of an entire arm, released as a 413 Da neutral to produce *m/z* 844.6 or as a protonated molecule detected at *m/z* 414.3, depending on the position of the charge at the time of the dissociation. This reaction could proceed via a 1,7-proton transfer from a methylene group to the central nitrogen atom (pathway (ii) in Scheme 2a). Two successive eliminations of isobutene were evidenced to occur from *m/z* 414.3 in MS^3 experiments and could account for the formation of *m/z* 358.2 and *m/z* 302.2, respectively. The *m/z* 844.6 ion could further eliminate up to four 2-methylprop-1-ene molecules, to generate *m/z* 788.5, *m/z* 732.5, *m/z* 676.4 and *m/z* 620.3, respectively (Fig. 2a). However, the same ion series could also result from the loss of an entire arm (413 Da) from A_{1-4}^+ ions. These ions were thus named C_i^+, *i* indicating the A_i^+ ion they arise from according to this reaction. Alternatively, C_i^+ ions could also be formed from A_{i+1}^+ ions upon the release of an entire arm containing both a *tert*-butyl- and an acid-terminated branch. Elimination of this 357 Da neutral would proceed according to the same mechanism as depicted in pathway (ii) of Scheme 2a. The complementary reaction would account for the *m/z* 358.2 product ion observed in Fig. 2a. Similarly, detection of a peak at *m/z* 302.2 assigned to $C_{14}H_{24}NO_6{}^+$ (Supplementary Table S1) suggests that C_i^+ product ions would also result from A_{i+2}^+ ions having eliminated a two acid-terminated arm. Finally, since all the C_{1-4}^+ product ions contain at least one acid-terminated branch, they could further eliminate a 72 Da neutral to yield corresponding D_{1-4}^+ ions (Fig. 2a). The proposed filiations have been validated by accurate mass measurements (Supplementary Table S1) and MS^3 experiments (data not shown).

Peaks observed in the low *m/z* range of the MS/MS spectrum could be explained by considering the previously described 72 Da neutral loss to occur from protonated arms containing one (*m/z* 358.2 → *m/z* 286.2) or two (*m/z* 302.2→ *m/z* 230.2 → *m/z* 158.1) acid-terminated branches. Formation of the *m/z* 342.3 product ion is depicted in Scheme 2a (pathway (iii)) to occur upon a 1,5-proton transfer at one of a central ester group in the precursor ion. The very low abundance of the complementary *m/z* 917.6 product ion suggests that *m/z* 342.3 would also be formed (according to the same mechanism) from any product ion still containing one arm with two *tert*-butyl terminations. In particular, cleavage of the ester bond within one arm of B_{1-4}^+ product ions would produce either C_{1-4}^+ ions or *m/z* 342.3, as supported by MS^3 experiments. Finally, the peak at *m/z* 242.2 would reveal an additional reaction from any ion possessing one arm with two acid-terminated branches. As shown in Scheme 2b for *m/z* 302.2, a proton transfer from one carboxylic acid function to the carbonyl oxygen of the second acidic group would produce *m/z* 242.2 upon elimination of ethene-1,1-diol (60 Da).

In summary, dissociation reactions observed during CID of the protonated dendrimer **P** provide straightforward structural information: (i) the number of 56 Da neutral losses from the precursor ion indicates the number of *tert*-butyl end-groups, (ii) the release of a 72 Da neutral consecutively to each 56 Da loss reveals the location of the *tert*-butyl group within a branch, (iii) the presence of an intact arm in any ion is diagnosed by the detection of *m/z* 414.3 and (iv) the release of an arm having eliminated one or two *tert*-butyl end-groups is characterized by product ions at *m/z* 358.2 and *m/z* 302.2, respectively. However, since targeted impurities were mostly ionized as doubly charged molecules upon electrospray (Fig. 1), the effect of charge state on dissociation reactions experienced by dendrimer **P** was investigated.

3.3. MS/MS study of doubly protonated *P*

Selection of doubly charged precursor ions was performed in a quadrupole analyzer which resolution was intentionally lowered to allow both the monoisotopic ion and its one ^{13}C counterpart

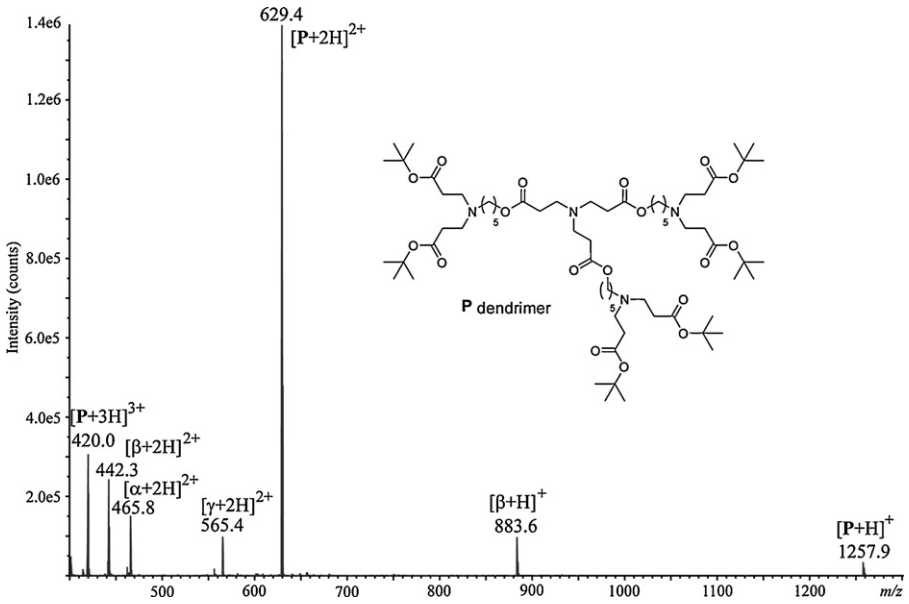

Fig. 1. Positive mode electrospray mass spectrum of the **P** sample. Perfect **P** molecule is observed as $[\mathbf{P}+n\mathrm{H}]^{n+}$ (n = 1–3) and three minor impurities (**α**, **β** and **γ**) were detected as singly and/or doubly protonated molecules. Inset: structure of precursor **P**.

to be simultaneously submitted to dissociation. Hence, in addition to information provided by accurate mass measurements, doubly charged products observed at *m/z* values lower than that of the precursor ion could readily be distinguished from singly charged ones based on their partial isotope pattern. CID data of $[\mathbf{P}+2\mathrm{H}]^{2+}$ at *m/z* 629.4 (Fig. 2b and Supplementary Table S2) mainly showed the production of A_i^{2+} ions (with i = 1–6) of similar relative abundance as compared to A_i^{+} ions in Fig. 2a, except for A_6^{2+} which exhibits a particularly high stability. B_i^{2+} ions were detected with low intensity, except for B_6^{2+} consistently with the high abundance of its proposed A_6^{2+} precursor. Although using a similar center-of-mass collision energy as compared to MS/MS of $[\mathbf{P}+\mathrm{H}]^{+}$, noticeable differences were observed in the low *m/z* range of the spectrum when activating the doubly charged precursor. Ions revealing the release of one arm containing two (*m/z* 414.3) or one (*m/z* 358.2) *tert*-butyl end-group (as well as their respective dissociation products) were hardly detected. The only clearly observed product ion was a protonated arm with both acid-terminated branches at *m/z* 302.2. Finally, singly charged A_i^{+} and C_i^{+} (but no B_i^{+}) could be detected with extremely low abundance when scrutinizing the high *m/z* range of the CID spectrum (inset of Fig. 2b). The *m/z* 692.3 product ion observed in the inset of Fig. 2b was also formed with low abundance from $[\mathbf{P}+\mathrm{H}]^{+}$ and could be accounted for by considering the cleavage of a central ester bond in A_4^{+}. As a result, due to the lack of product ions arising from arm detachment, CID data from the doubly protonated precursor appeared to be less informative as compared to MS/MS of $[\mathbf{P}+\mathrm{H}]^{+}$.

3.4. Structural characterization of defective molecules.

3.4.1. Impurity α

Compared to the perfect dendrimer **P**, **α** showed a mass default of 327 Da. Accurate mass measurements performed for $[\boldsymbol{\alpha}+2\mathrm{H}]^{2+}$ suggested a $C_{48}H_{89}N_3O_{14}{}^{2+}$ elementary composition (*m/z* 468.8166; error: −0.2 ppm). When submitted to CID, $[\boldsymbol{\alpha}+2\mathrm{H}]^{2+}$ was shown to eliminate up to four 56 Da neutrals, giving rise to a A_i^{2+} ion series indicating a total of four *tert*-butyl functions in the precursor ion (Fig. 3).

In the expected B_i^{2+} product ion series, only B_4^{2+} could be detected at *m/z* 317.7. Consistently with the reference behavior of doubly protonated molecules (Fig. 2b), the last B_i^{2+} congener is the most abundant one. The absence of B_{1-3}^{2+} in the CID spectrum of $[\boldsymbol{\alpha}+2\mathrm{H}]^{2+}$ precursor would be due to the low abundance of A_{1-3}^{2+}, as compared to the case of **P**. The ion at *m/z* 302.2, assigned to a protonated arm with both acid-terminated branches, revealed that the **α** molecule contained at least one intact arm. The peak at *m/z* 323.7 would result from the elimination of a 60 Da neutral from A_4^{2+} at *m/z* 353.7, that is, ethene-1,1-diol as depicted in Scheme 2b. Based on this assumption, it could be concluded that A_4^{2+} contains two acid-terminated branches within the same arm. From accurate mass measurements (Supplementary Table S3) as well a MS^3 experiments, the doubly charged molecule detected at *m/z* 310.7 could be considered as the result of a $C_4H_6O_2$ (86 Da) loss from A_4^{2+}. As compared to the elimination of acrylic acid (72 Da) experienced by A_4^{2+} to produce B_4^{2+} ions, release of this 86 Da neutral assigned to a methacrylate molecule would reveal that one branch in A_4^{2+} at *m/z* 353.7 contains a methyl ester function. However, due to the lack of informative product ions generated from the dissociation of this doubly charged precursor, location of this defective branch could not be precisely defined from the sole CID data.

In summary, MS/MS data together with accurate mass measurements allowed to conclude that the **α** impurity would consist of a dendritic molecule with two arms, a total of four *tert*-butyl-terminated branches and one methyl-terminated branch. As a result, a branch should be connected to the central nitrogen atom, but from MS/MS data shown in Fig. 3, it cannot be concluded whether this branch is methyl- or *tert*-butyl-terminated. With regard to the structure of impurities characterized in the acid-terminated dendrimer sample, **α** might well be considered as the precursor of impurity I (Scheme 1), assuming the defective branch in **α** would be part of an arm (as shown in the inset of Fig. 3). In our previous study, the presence of impurity I in the acidic-terminated dendrimers sample was considered to result from acidolysis upon TFA treatment of the ester group within one arm of the *tert*-butyl ester-terminated precursor **P**. Although this assumption could not be totally rejected, detection of impurity **α** in the **P** sample clearly indicates an alternative defective reaction in the dendrimer synthesis, i.e., a subquantitative success of either transesterification in the second step or of activation of carboxylic functions in step one (Scheme 1).

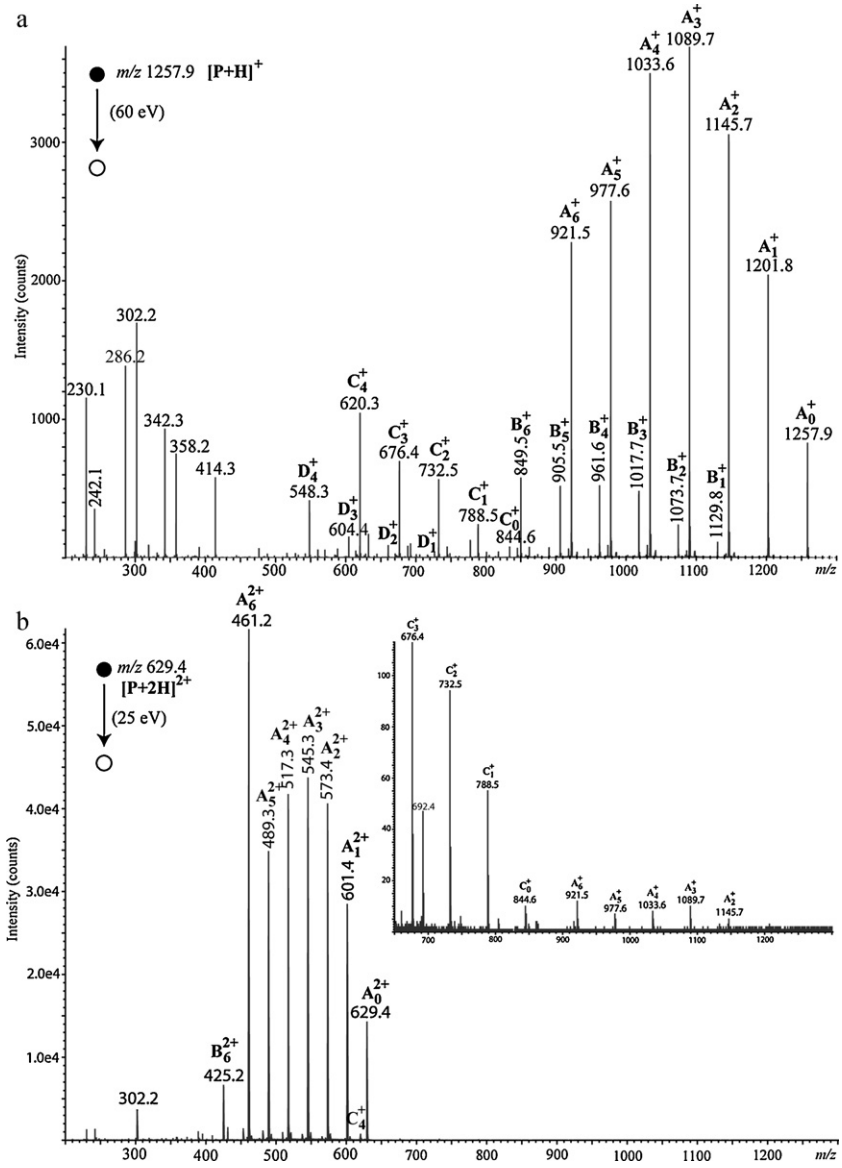

Fig. 2. CID spectrum of (a) $[\mathbf{P}+H]^+$ at *m/z* 1257.9 using a 60 eV collision energy and (b) $[\mathbf{P}+2H]^{2+}$ at *m/z* 629.4 using a 25 eV collision energy (laboratory frame). Inset: expansion of the 650–1300 *m/z* range.

3.4.2. Impurity **β**

In contrast to **α**, structural information for **β** could be obtained from CID data of both singly and doubly protonated molecules. According to CID of $[\mathbf{\beta}+H]^+$ (*m/z* 883.6006: $C_{46}H_{83}N_4O_{12}^+$; error: +0.5 ppm), impurity **β** contains four *tert*-butyl ester groups. These functions could be eliminated as 2-methylprop-1-ene molecules either from *m/z* 883.6, giving rise to A^+_{1-4} product ions, or after the precursor ion has released a HCN neutral, producing the so-called $(A'_{1-4})^+$ ions (Fig. 4). Although no B_i^+ ions could be detected in the CID spectrum of $[\mathbf{\beta}+H]^+$, presumably due to the low abundance of their respective A_i^+ precursor, $(A'_i)^+$ ions were observed to eliminate a 72 Da neutral to produce $(B'_i)^+$ ions (not annotated in Fig. 4 for sake of clarity but accurately mass measured as shown in Supplementary Table S4). It could therefore be concluded that each *tert*-butyl ester function was located at the end of a branch in the precursor ion. In addition, detection of an *m/z* 414.3 product ion would confirm at least one intact arm in the precursor ion structure. Two additional ion series spaced by 56 Da could also be noticed. The first series, starting with *m/z* 782.5 (which further eliminates up to three 2-methylprop-1-ene molecules to yield *m/z* 726.5, *m/z* 670.4 and *m/z* 614.3, respectively) would be formed upon elimination of a $C_4H_{10}O$ neutral from $(A'_0)^+$. As evidenced in MS^3 experiments, the first congener of the second series at *m/z* 756.5 (from which three successive 56 Da losses would respectively yield *m/z* 700.5, *m/z* 644.4 and *m/z* 588.3) would also arise from the dissociation of $(A'_0)^+$ at *m/z* 856.6 (i.e., loss of a 100 Da neutral). These two ion series would arise from new dissociation reactions only proceeding from product ions which do no longer contain the cyano group. This suggests that this structural defect is located in a branch which is part of an arm, in contrast to a branch directly connected to the central nitrogen core. Accordingly, and combined with structural features previously validated for impurities found in the final dendrimer sample (Scheme 1), **β** could be considered as the precursor of impurity II.

Assuming such a structure for **β** (top of Fig. 4) would allow formation of product ions at *m/z* 782.5 and *m/z* 756.5 to be accounted for. Elimination of HCN from $[\mathbf{\beta}+H]^+$ to generate $(A'_0)^+$ at *m/z* 856.6 would be proton-induced due to the basicity of the cyano group. The release of $(CH_3)_3C–OH$ from $(A'_0)^+$ would then occur via a 1,6-proton transfer (Scheme 3, left-hand part). Alternatively, after a

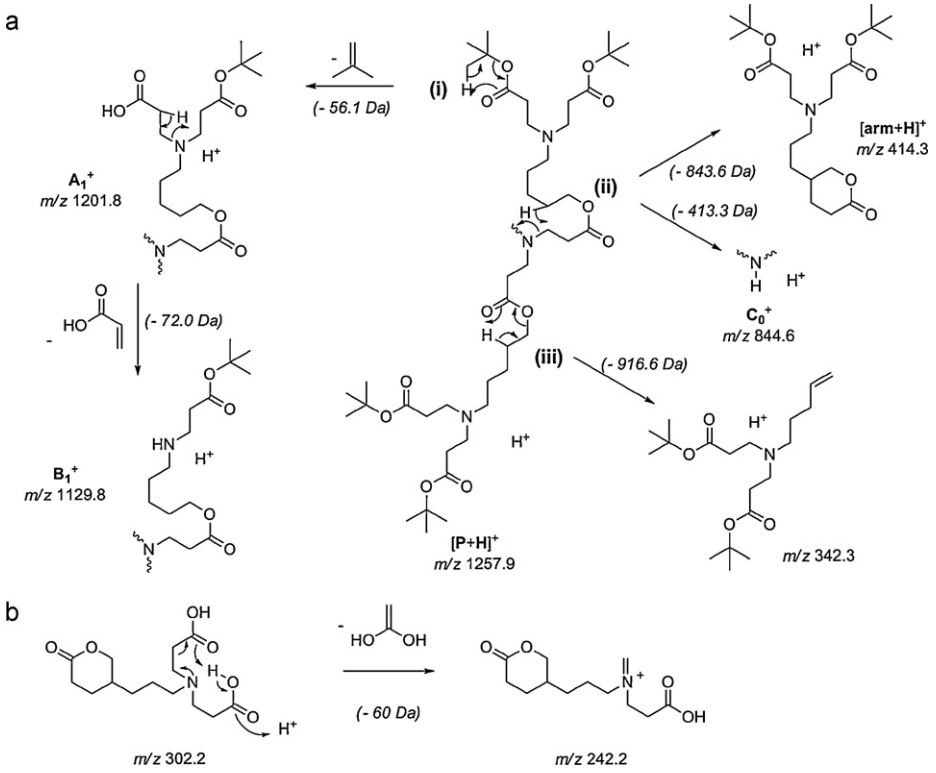

Scheme 2. (a) Proposed pathways for the dissociation of $[\mathbf{P}+H]^+$ at *m/z* 1257.9: (i) elimination of 2-methylprop-1-ene (56 Da) yielding A_1^+ at *m/z* 1201.8, followed by the release of acrylic acid (−72 Da) to produce B_1^+ at *m/z* 1129.8; (ii) detachment of an entire arm as a neutral molecule (yielding C_0^+ at *m/z* 844.6) or as a protonated molecule at *m/z* 414.3; (iii) formation of *m/z* 342.3 upon a 1,5-proton transfer at a central ester group. b) Mechanism proposed to account for the loss of ethene-1,1-diol (60 Da) from *m/z* 302.2 to produce *m/z* 242.2.

1,3-proton transfer has allowed the double bond to be relocated in the intact branch, transfer of a proton from the *tert*-butyl group to the positively charged nitrogen atom would induce a concerted loss of isobutene and carbon dioxide (Scheme 3, right-hand part).

CID data from $[\boldsymbol{\beta}+2H]^{2+}$ are consistent with the proposed structure but were found to be less informative as compared to results obtained for the singly charged molecule. When doubly protonated, the precursor ion (*m/z* 442.3041: $C_{46}H_{84}N_4O_{12}{}^{2+}$; error: +0.9 ppm) was observed to release up to four 56 Da neutrals, giving rise to A_{1-4}^{2+} product ions, with A_4^{2+} of particularly high abundance (Supplementary Fig. S1). Based on accurate mass measurements (Supplementary Table S5) and MS^3 experiments, the peak at *m/z* 316.7 would reveal the elimination of a HCN molecule from A_4^{2+}. A careful examination of the MS/MS spectrum indicates that the release of HCN also proceeds from other A_i^{2+} product ions (to yield *m/z* 344.7 from A_3^{2+}, *m/z* 372.7 from A_2^{2+}, and *m/z* 400.8 from A_1^{2+}). In addition to the protonated acid-terminated arm at *m/z* 302.2, the low *m/z* range of the CID spectrum exhibits three doubly charged

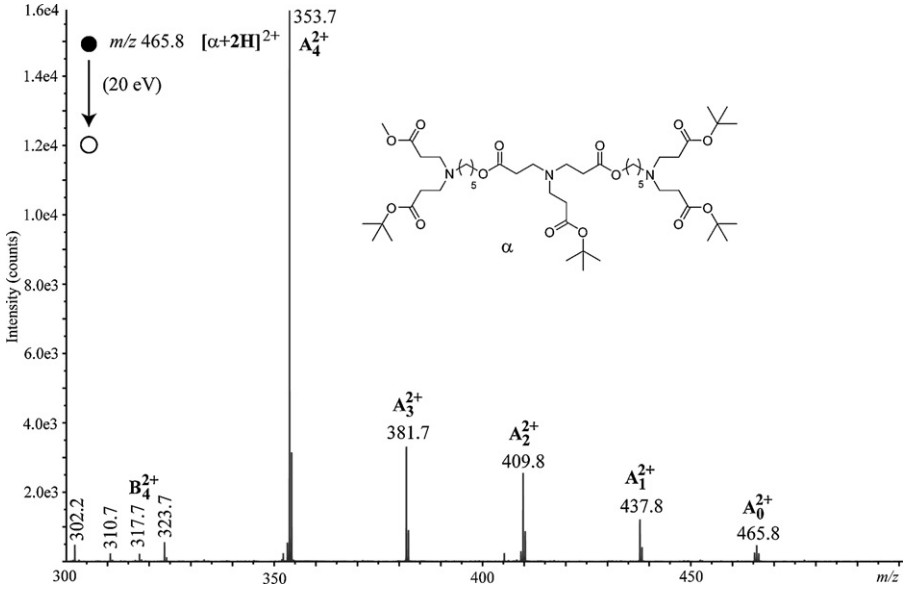

Fig. 3. CID spectrum of $[\boldsymbol{\alpha}+2H]^{2+}$ at *m/z* 465.8 using a 20 eV collision energy (laboratory frame). Inset: proposed structure for **α**.

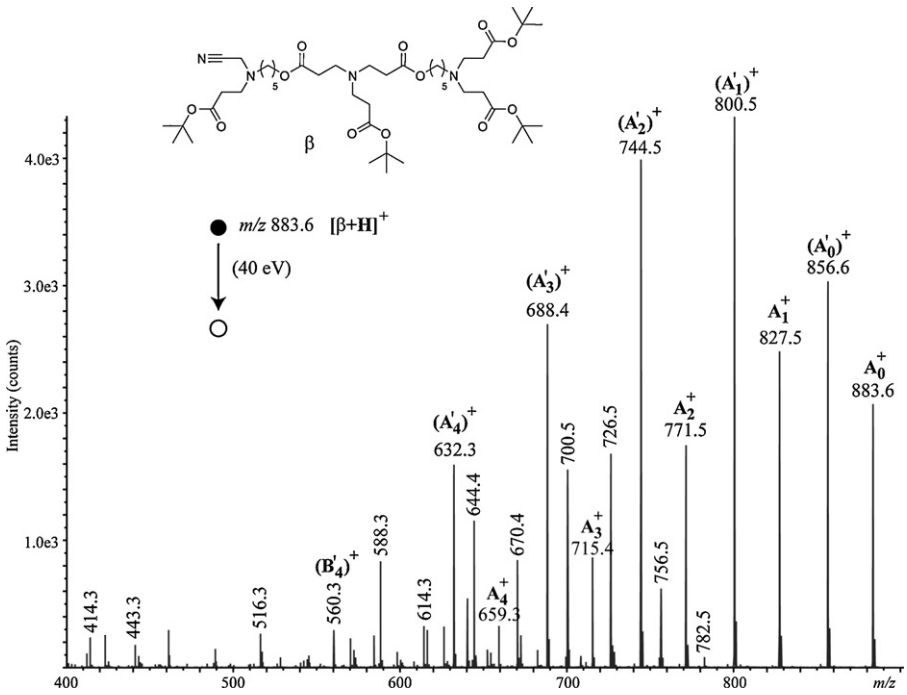

Fig. 4. CID spectrum of [**β**+H]+ at *m/z* 883.6 using a 40 eV collision energy (laboratory frame). Top: proposed structure for **β**.

molecules at *m/z* 294.7, *m/z* 286.7 and *m/z* 264.7. The loss of ethene-1,1-diol from *m/z* 316.7 could account for the formation of *m/z* 286.7. This result is consistent with the presence of one arm with two acid-terminated branches in the *m/z* 316.7 product ion. Elimination of CO_2 from *m/z* 316.7 and *m/z* 286.7 would result in the formation of *m/z* 294.7 and *m/z* 264.7, respectively, similarly to the process depicted in Scheme 3 (right-hand side) with a 1,5 transfer of the acidic proton to the positively charged nitrogen formed upon loss of HCN. An alternative pathway to generate *m/z* 264.7 is the loss of ethane-1,1-diol from *m/z* 294.7.

In contrast to the case of **α** for which only the doubly protonated precursor could be studied by MS/MS, the defective structural moiety could clearly be located in **β** based on CID data obtained for the singly charged molecule. This molecule could be validated as the precursor of impurity II in the acid-terminated dendrimer sample. As a result, the defective arm in impurity II should not be exclusively assigned to acidolysis of one ester group of the intact precursor **P** submitted to TFA treatment. Once again, previous steps of the dendrimer synthesis should also be questioned.

3.4.3. Impurity γ

MS/MS pattern (Fig. 5) combined with accurate mass measurements (Supplementary Table S6) allowed a straightforward characterization of the impurity **γ**, although it was mainly produced as a doubly protonated molecule [**γ**+2H]$^{2+}$ at *m/z* 565.4. The $C_{59}H_{110}N_4O_{16}{}^{2+}$ composition (*m/z* 565.3953; error: −0.5 ppm) determined for the precursor ion suggests that one entire branch is missing compared to **P**. This is consistent with the five 56 Da neutral loss sequence observed to produce *m/z* 537.4, *m/z* 509.3, *m/z* 481.3, *m/z* 453.3 and *m/z* 425.2 (Fig. 5). In contrast to doubly protonated molecules studied so far, A_i^{2+} product ions generated from [**γ**+2H]$^{2+}$ were all observed to further eliminate a 72 Da neutral to

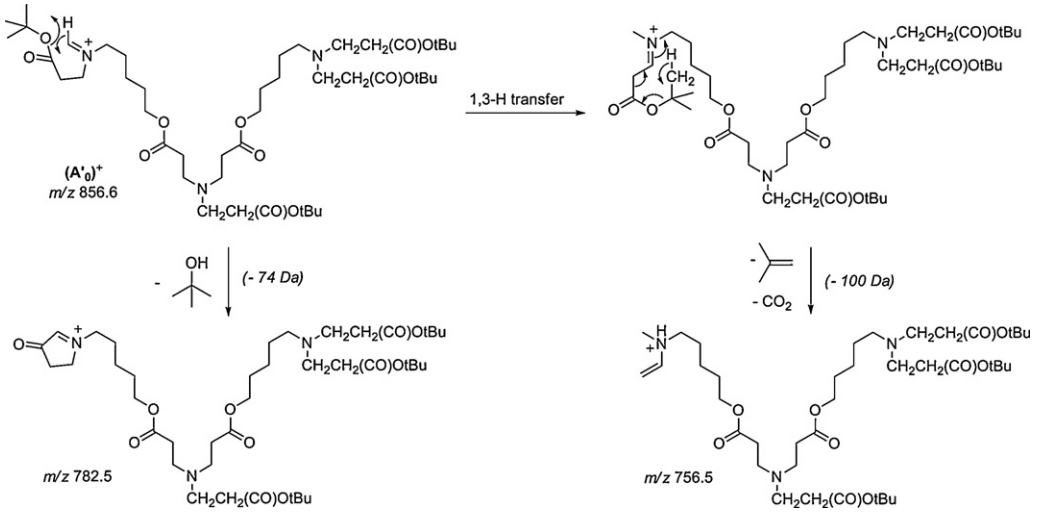

Scheme 3. Proposed pathways for the formation of two additional ion series during CID of [**β**+H]+, starting from *m/z* 782.5 formed after elimination of *tert*-butanol from $(A'_0)^+$, or starting from *m/z* 756.5 generated after a concerted loss of isobutene and carbon dioxide from $(A'_0)^+$.

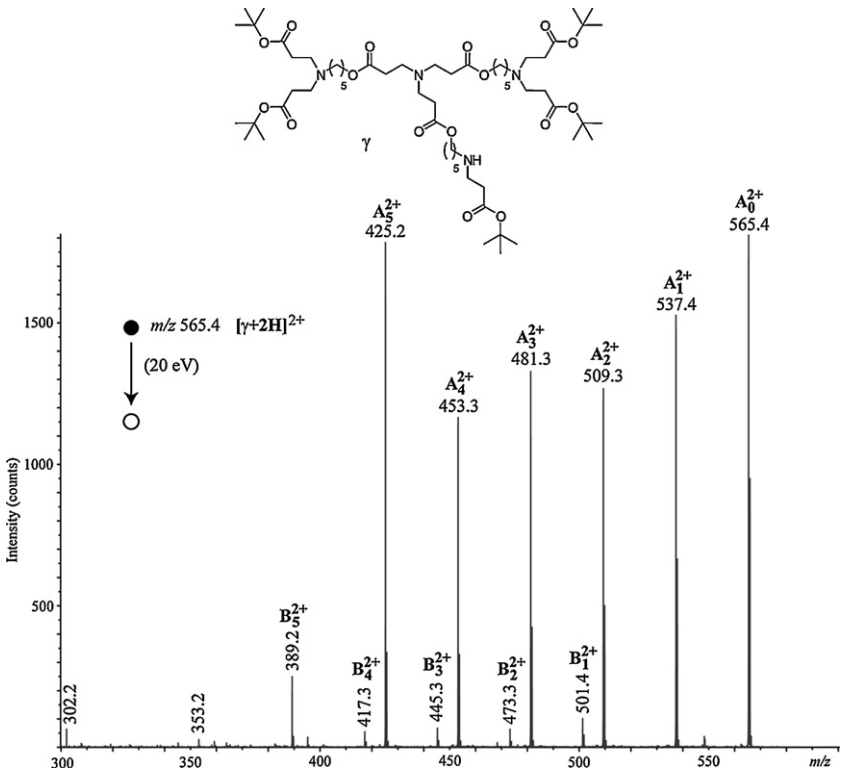

Fig. 5. CID spectrum of $[\gamma+2H]^{2+}$ at *m/z* 565.4 using a 20 eV collision energy (laboratory frame). Top: proposed structure for **γ**.

yield the B_i^{2+} ions. This is probably due to the lack of competitive dissociation reactions in the case of **γ**. In addition, the same 72 Da neutral loss also occurs from B_5^{2+}, to produce *m/z* 353.2. Finally, *m/z* 302.2 was assigned to the protonated acid-terminated arm. All these findings allowed the structure shown on top of Fig. 5 to be readily proposed for the impurity **γ**.

Since no impurity arising from deprotection of the ester terminals in **γ** could be detected in the final acid-terminated dendrimer sample, **γ** was suspected to have been thoroughly modified during the TFA treatment. In particular, since sample **P** was not shown to contain any molecule corresponding to the *tert*-butyl-ester form of impurity III previously identified in the final dendrimer sample (Scheme 1), acidolysis of the N–C bond involving the central nitrogen atom in **γ** was envisaged. Such acid-catalyzed N–C bond cleavage was previously reported for alkoxyamines in the presence of strong acids such as TFA, yielding a secondary amine function and elimination of the *tert*-butyl moiety initially linked to the nitrogen atom [17]. A similar acidolysis might well be envisaged in **γ**, owing to both the basicity of the core tertiary amine function and the stability of the released lactone (413 Da). Although probably proceeding at a much lower rate than deprotection of the terminal acidic functions, due to steric hindrance which limits accessibility of TFA to the core amine function, this secondary reaction would allow **γ** to be considered as the precursor of III.

4. Conclusion

The fragmentation behavior of a *tert*-butyl-terminated poly(amino)ester dendrimer was established, based on collision-induced dissociation of its protonated form. Due to the high symmetry of the dendritic precursor ion, sequential neutral losses were shown to occur, which could hence be readily used as a reference to identify any defective molecules present as trace impurities in the sample. Combined with accurate mass data, this structural MS/MS approach was shown to be very efficient, particularly when applied to singly charged molecules for which complementary information could be obtained from distinct dissociation reactions. Location of defective moiety in those impurities which were mainly ionized in the +2 charge state was sometimes more puzzling but could be established based on the structure of impurities detected in the next step of the synthesis. Propagation of main structural deviations could be demonstrated from the *tert*-butyl ester bearing precursor **P** to the acid-terminating poly(amino)ester dendrimer **D**. This result suggests that deprotection reaction using TFA in the last step of our synthesis of poly(amino)ester dendrimers is mild enough to keep the dendrimer arms intact, in spite of the labile character of the ester linkage. The origin of defective moieties found in impurities of both **P** and **D** samples, such as the methoxy and the cyano groups, needs to be further investigated in preceding steps of the synthesis in the view to understand their formation and hence to prevent their appearance during the synthesis of poly(amino)ester dendrimers.

Acknowledgments

L. Charles acknowledges support from Spectropole, the Analytical Facility of Aix-Marseille University, by allowing a special access to the instruments purchased with European Funding (FEDER OBJ2142-3341). This work is under the frame of the COST Action TD0802 “Biological Applications of Dendrimers” and partly supported by ERA-Net EURONANOMED European Research Project DENANORNA.

Appendix A. Supplementary data

Supplementary data associated with this article can be found, in the online version, at doi:10.1016/j.ijms.2011.07.021.

References

[1] D.A. Tomalia, A.M. Naylor, W.A. Goddard, Starburst dendrimers—molecular-level control of size, shape, surface-chemistry, topology, and flexibility from atoms to macroscopic matter, Angew. Chem. Int. Ed. 29 (1990) 138–175.

[2] O.L.P. De Jesus, H.R. Ihre, L. Gagne, J.M.J. Frechet, F.C. Szoka, Polyester dendritic systems for drug delivery applications: in vitro and in vivo evaluation, Bioconjug. Chem. 13 (2002) 453–461.

[3] H.R. Ihre, O.L.P. De Jesus, F.C. Szoka, J.M.J. Frechet, Polyester dendritic systems for drug delivery applications: design, synthesis, and characterization, Bioconjug. Chem. 13 (2002) 443–452.

[4] B. Buschhaus, F. Hampel, S. Grimme, A. Hirsch, Metal-induced chiral folding of depsipeptide dendrimers, Chem. Eur. J. 11 (2005) 3530–3540.

[5] C. Bouillon, G. Quelever, L. Peng, Efficient synthesis of esters containing tertiary amine functionalities via active cyanomethyl ester intermediates, Tetrahedron Lett. 50 (2009) 4346–4349.

[6] C. Bouillon, A. Tintaru, V. Monnier, L. Charles, G. Quelever, L. Peng, Synthesis of poly(amino)ester dendrimers via active cyanomethyl ester intermediates, J. Org. Chem. 75 (2010) 8685–8688.

[7] A. Tintaru, V. Monnier, C. Bouillon, R. Giordanengo, G. Quelever, L. Peng, L. Charles, Structural characterization of poly(amino)ester dendrimers and related impurities by electrospray tandem mass spectrometry, Rapid Commun. Mass Spectrom. 24 (2010) 2207–2216.

[8] J.W. Weener, J.L.J. van Dongen, E.W. Meijer, Electrospray mass spectrometry studies of poly(propylene imine) dendrimers: probing reactivity in the gas phase, J. Am. Chem. Soc. 121 (1999) 10346–10355.

[9] S.A. McLuckey, K.G. Asano, T.G. Schaaff, J.L. Stephenson, Ion trap collisional activation of protonated poly(propylene imine) dendrimers: generations 1–5, Int. J. Mass Spectrom. 195 (2000) 419–437.

[10] A. Adhiya, C. Wesdemiotis, Poly(propylene imine) dendrimer conformations in the gas phase: a tandem mass spectrometry study, Int. J. Mass Spectrom. 214 (2002) 75–88.

[11] M. He, S.A. McLuckey, Tandem mass spectrometry of half-generation PAMAM dendrimer anions, Rapid Commun. Mass Spectrom. 18 (2004) 960–972.

[12] C.L. Mazzitelli, J.S. Brodbelt, Investigation of silver binding to polyamidoamine (PAMAM) dendrimers by ESI tandem mass spectrometry, J. Am. Soc. Mass Spectrom. 17 (2006) 676–684.

[13] R. Giordanengo, M. Mazarin, J.Y. Wu, L. Peng, L. Charles, Propagation of structural deviations of poly (amidoamine) fan-shape dendrimers (generations 0–3) characterized by MALDI and electrospray mass spectrometry, Int. J. Mass Spectrom. 266 (2007) 62–75.

[14] J. Subbi, R. Aguraiuja, R. Tanner, V. Allikmaa, M. Lopp, Fragmentation of poly(amidoamine) dendrimers in matrix-assisted laser desorption, Eur. Polym. J. 41 (2005) 2552–2558.

[15] L. Charles, Influence of internal standard charge state on the accuracy of mass measurements in orthogonal acceleration time-of-flight mass spectrometers, Rapid Commun. Mass Spectrom. 22 (2008) 151–155.

[16] K. Chaicharoen, M.J. Polce, A. Singh, C. Pugh, C. Wesdemiotis, Characterization of linear and branched polyacrylates by tandem mass spectrometry, Anal. Bioanal. Chem. 392 (2008) 595–607.

[17] T. Trimaille, K. Mabrouk, V. Monnier, L. Charles, D. Bertin, D. Gigmes, SG1-functionalized peptides as precursors for polymer–peptide conjugates: a straightforward approach, Macromolecules 43 (2010) 4864–4870.